On the one hand, the greatest part of the equi-intensity curves in Fig. 4 and the TCD curves in Fig. 3 are measured in regions with $q > 1/R_0$. Here (3), which the calculations are based on, is never valid, and the angular distribution of diffuse scattering should be changed. On the other hand, since the defects are very large, surface relaxation of the displacement fields and dynamical effects of X-ray diffraction will be of importance. One disadvantage of this method is the domination of the diffuse scattering caused by the larger defects in the case of a mixture of defects of different size. In the case described the small precipitates, observed by TEM, were not detectable by X-ray measurements.

Nevertheless, the results presented show that it is possible to characterize defects even up to 1 μm in size by the non-destructive method of X-ray diffuse scattering with TCD and by calculations based on the simple theory of Huang scattering.

The authors wish to thank E. Bugiel for the TEM results obtained at the HVEM of the IFE Halle and Dr C. Becker, Dr R. M. Imamov and Dr A. A. Zavyalova for their interest in the work, helpful discussions and for carefully reading the manuscript.

References

DEDERICHS, P. H. (1971). *Phys. Rev. B*, **4**, 1041-1050.

DEDERICHS, P. H. (1973). *J. Phys. F*, **3**, 471-496.

EHRHARD, P. & SCHILLING, W. (1974). *Phys. Rev. B*, **8**, 2604-2621.

IIDA, A. (1979). *Phys. Status Solidi A*, **54**, 701-706.

IIDA, A. & KOHRA, K. (1979). *Phys. Status Solidi A*, **51**, 533-542.

LAL, K. (1981). *Proc. Indian Nat. Sci. Acad. Part A*, **47**, 20-46.

LARSON, B. C. (1975). *J. Appl. Cryst.* **5**, 150-160.

LARSON, B. C. & BARHORST, J. F. (1981). *Defects in Semiconductors*, pp. 151-162. Amsterdam: North-Holland.

LARSON, B. C. & SCHMATZ, W. (1974). *Phys. Rev. B*, **10**, 2307-2314.

LARSON, B. C. & YOUNG, F. W. JR (1973). *Z. Naturforsch. Teil A*, **28**, 626-632.

LOHSTÖTER, H., SPALT, H. & PEISEL, H. (1972). *Phys. Rev. Lett.* **29**, 224-226.

MAYER, W. & PEISEL, H. (1982). *J. Nucl. Mater.* **108 & 109**, 627-634.

PATEL, J. R. (1975). *J. Appl. Cryst.* **8**, 186-191.

RICHTER, H., MAI, M., KIRSCHT, F. G. & GAWORZEWSKI, P. (1983). *Physica (Utrecht)*, **116B**, 162.

SPALT, H. (1970). *Z. Angew. Phys.* **29**, 269-276.

THOMAS, J. E., BALDWIN, T. O. & DEDERICHS, P. H. (1971). *Phys. Rev. B*, **3**, 1167-1173.

ZAUMSEIL, P. & WINTER, U. (1982*a*). *Phys. Status Solidi A*, **70**, 471-496.

ZAUMSEIL, P. & WINTER, U. (1982*b*). *Phys. Status Solidi A*, **73**, 455-466.

Acta Cryst. (1985). A**41**, 227-232

Three-Crystal Diffractometry in Grazing Bragg–Laue Geometry

BY A. M. AFANAS'EV,* P. A. ALEKSANDROV,* R. M. IMAMOV, A. A. LOMOV & A. A. ZAVYALOVA

Institute of Crystallography of the USSR Academy of Sciences, Leninsky prospect 59, *Moscow* 117333, *USSR*

(*Received* 28 *March* 1984; *accepted* 19 *November* 1984)

Abstract

Three-crystal X-ray diffractometry (TCD) in grazing Bragg–Laue geometry has been experimentally realized for the first time. Theoretical simulations for the angular position and intensity of the main peak and the pseudopeak on TCD spectra have been obtained. It was established that TCD in grazing Bragg–Laue geometry has the following peculiarities: (1) the angular position and intensity of the main peak on the spectra depend on the sign of the deviation angle; (2) the main peak vanishes completely at negative deviation angles reaching the critical value; (3) the intensity of the main peak in grazing Bragg–Laue geometry is increased approximately by a factor of 10^2 (compared to symmetrical Bragg diffraction geometry). The above peculiarities were predicted theoretically and confirmed by experimental studies on ideal Si crystals.

Introduction

The method of three-crystal diffractometry (TCD) for the analysis of the angular distribution of diffracted X-rays (Eisenberger, Alexandropoulos & Platzman, 1972; Larson & Schmatz, 1974, 1980; Haubold & Martinsen, 1978; Iida & Kohra, 1979; Iida, 1979; Afanas'ev, Koval'chuk, Lobanovich, Imamov, Aleksandrov & Melkonyan, 1981; Zaumseil & Winter, 1982) is an effective method for investigating distortions in a crystal, in particular in its subsurface layers. TCD was traditionally used to measure diffuse scattering due to the defects of the crystal lattice (Larson & Schmatz, 1974, 1980; Ehrhart, 1978; Haubold & Martinsen, 1978; Iida & Kohra, 1979; Iida, 1979; Zaumseil & Winter, 1982). Recently some authors (Afanas'ev, Koval'chuk, Lobanovich, Imamov,

* Kurchatov Institute of Atomic Energy, Kurchatov square 46, Moscow 123182, USSR.

0108-7673/85/030227-06$01.50

Aleksandrov & Melkonyan, 1981; Afanas'ev, Aleksandrov & Melkonyan, 1981; Afanas'ev, Aleksandrov, Imamov, Lomov & Zavyalova, 1983, 1984; Yakimov, Chaplanov, Afanas'ev, Aleksandrov, Imamov & Lomov, 1984) have shown theoretically and experimentally the possibility of obtaining important information on the structural perfection of subsurface layers from the angular dependence of the parameters of the main peak and pseudopeaks. The papers (Afanas'ev *et al.*, 1983, 1984; Yakimov *et al.*, 1984) report a high sensitivity of the TCD method, which allows damaged layers with thicknesses of the order of 1 nm to be observed.

The diffraction arrangement, shown in Fig. 1, is very convenient for investigating thin subsurface layers. In this geometry X-rays fall on a crystal at grazing angle Φ_0 and are diffracted by a lattice plane with its normal vector making a small angle of disorientation $|\varphi|$. Depending on Φ_0, either the diffraction in Laue geometry ($\Phi_0 > 2|\varphi| \sin\theta_B$) or in Bragg geometry ($\Phi_0 < 2|\varphi| \sin\theta_B$) can be realized (Aleksandrov, Afanas'ev & Stepanov, 1984).

The peculiarities of Bragg-Laue diffraction in a two-crystal arrangement with a simultaneous analysis of the angular dependence of the photoelectron yield were investigated in previous papers (Afanas'ev, Imamov, Maslov & Pashaev, 1983, 1984). In the case of diffraction in the Bragg geometry we have a large reflection coefficient (of the order of unity), and, therefore, a possibility arises for measuring TCD curves at large deviation from the exact Bragg position. Diffraction at grazing angles of incidence of X-rays ensures a small extinction depth, so that it permits the investigation of thinner layers of crystals.

A TCD investigation in this geometry has been performed for the first time, and the present paper is devoted to finding out the basic physical features of the diffraction process. The most important peculiarity of diffraction in this arrangement consists in the fact that at small deviations from the Bragg condition the exit angle of diffracted rays Φ_h changes significantly. The change of deviation angle α by several seconds changes Φ_h by several degrees, which can influence significantly the diffraction geometry. Moreover, at such deviations from the Bragg condition, regardless of the initial geometry of diffraction, diffracted waves directed both into the crystal and outward from it are always formed. This circumstance compelled us to define the given diffraction arrangement as the case of grazing Bragg-Laue diffraction. Here rather important dependences of the position and intensity of the main peak on α are observed.

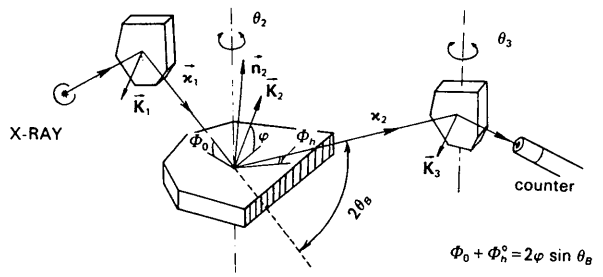

Fig. 1. The arrangement of the TCD method in the grazing Bragg-Laue geometry.

The diffraction at grazing angles was used previously by several workers. In works on the structure studies of monolayers of adsorbed atoms and phase transitions in them (Birgenvau, Hammous, Heiney & Stephaus, 1980; Nielsen, Als-Nielsen, Bohr & McTague, 1981), grazing angles were necessary to lower the background due to X-rays scattered from the substrate. Marra, Eisenberger & Cho (1979) suggested an arrangement in which specular reflection occurred simultaneously with diffraction. Under these conditions it became possible to diminish still more the background due to the substrate. This idea was later used in studies on the reconstruction of Ge surfaces (Eisenberger & Marra, 1981) and Au surfaces (Robinson, 1983) as well as in studies on melting processes of Pb layers on Cu surfaces (Marra, Fuoss & Eisenberger, 1982), although the use of specular reflection is not that critical for high-power X-ray sources. In our previous paper (Afanas'ev & Melkonyan, 1983), a correlation was found between the deviation angle α and the exit angle Φ_h of diffracted waves, which allows a considerable simplification of the experiments in which both the Bragg diffraction and specular reflection took place (Golovin & Imamov, 1983*a*, *b*).

In the present study the specular reflection phenomenon is not used. Diffraction in the Bragg geometry is realized owing to small disorientation φ ($\varphi < 0$) (of the order of several degrees) and the deviation from the Bragg angle. Here angles Φ_0 and Φ_h along with φ have the values of several degrees. This fact changes qualitatively the experiment. Its realization becomes much simpler, allowing the thinnest layers on the crystal surface to be studied using conventional X-ray sources.

Theory

Let us consider X-ray diffraction in the geometry shown in Fig. 1. Depending on the angles of incidence of X-rays on the crystal (Φ_0 and θ_B) the diffracted wave can propagate either outward from the crystal or inward. Sometimes both waves are formed. This takes place when the angle Φ_0 is comparable with the critical angle of specular reflection Φ_c, which for a Si crystal is 13′, and for Ge and GaAs crystals ~18′. In the present study we shall consider only the case when the disorientation angle $|\varphi|$ is much larger than Φ_c, so that either the incident or the diffracted wave makes an angle with the surface that is much larger than the angle of specular reflection. The case with angles Φ_0, $|\varphi| < \Phi_c$ requires not only more compli-

cated calculations but also experimental devices of higher precision.

If X-rays fall on the studied crystal at an exact Bragg angle, when $\theta_2 = 0$ (Fig. 1)

$$\alpha = \frac{(\varkappa_1 + \mathbf{K}_2)^2 - \varkappa_1^2}{\varkappa_1^2} = -2(\sin\theta_B)\theta_2 = 0, \quad (1)$$

then diffraction in the Laue geometry is realized at grazing angles

$$\Phi_0 > |\Psi|, \quad \text{where } \Psi = 2\varphi \sin\theta_B \quad (2)$$

and in the Bragg geometry at angles

$$\Phi_0 < |\Psi|. \quad (3)$$

Here the exit angle for the diffracted wave

$$\Phi_{h/\alpha=0} \equiv \Phi_h^0 = |\Psi| - \Phi_0. \quad (4)$$

At a deviation from the exact Bragg angle, $\alpha \neq 0$, the angle Φ_h changes according to the equation (see Afanas'ev & Melkonyan, 1983):

$$\Phi_h^2 = (\Phi_h^0)^2 - \alpha. \quad (5)$$

The change of angle α by several minutes corresponds to the change of Φ_h by several degrees. As a result of this, it is not only the diffraction geometry that can change from the Laue case to the Bragg case and *vice versa*, but also the asymmetry factor $\beta = \Phi_0/\Phi_h$ will change within the same geometry with change in parameters. For instance, at $\alpha > (\Phi_h^0)^2$ diffraction scattering does not occur, nevertheless, diffraction processes cause a significant change of X-ray field near the surface, which can influence the yield of secondary radiation (fluorescence, photoelectrons).

In the TCD method the specimen is fixed at a certain position and the angular distribution of diffracted X-rays is studied by making use of the third analyzer crystal. The spectrum usually contains three peaks: the main peak, the pseudopeak and the diffuse peak [see Fig. 2 and Iida & Kohra (1979), Afanas'ev, Koval'chuk, Lobanovich, Imamov, Aleksandrov & Melkonyan (1981)].

Let us find the positions of these peaks for the geometry considered. All three crystals are initially placed in such order that all the three vectors of the reciprocal lattices $\mathbf{K}_1$, $\mathbf{K}_2$ and $\mathbf{K}_3$ are parallel to each other. Then, the second crystal is rotated by angle θ_2 around axis $\mathbf{n}$ perpendicular to the scattering plane. Here, for beam $\varkappa_1$, falling on the second crystal, the exact Bragg condition is no longer fulfilled. The beam diffracted by the second crystal will not correspond to the exact Bragg angle for the third crystal either. However, this discrepancy can be eliminated by rotating the third crystal around the same axis $\mathbf{n}$. The corresponding rotation angle can be readily obtained

$$\theta_m = \frac{2|\Psi|\theta_2}{\Phi_h + \Phi_h^0} \equiv \frac{2|\varphi|}{[(\Phi_h^0)^2 - \alpha]^{1/2} + \Phi_h^0}\theta_2 \equiv \frac{|\Psi|\delta}{\sin 2\theta_B} \quad (6)$$

where $\delta = \Phi_h - \Phi_h^0$. The angular position of the main peak on TCD spectra will thus correspond to such a rotation of the third crystal.

The pseudopeak is due to the beams that fall on the first crystal at a non-exact Bragg angle and still satisfy the exact Bragg condition for diffraction on the second crystal. The corresponding rotation angle of the third crystal

$$\theta_p = \theta_2 \quad (7)$$

determines the angular position of the pseudopeak on the TCD spectrum. The diffuse peak in this scattering geometry is greatly blurred (this point will be considered in detail in the next paper).

The intensity of the main peak under the condition

$$|\alpha| \gg |\chi_h| \quad (8)$$

can be calculated in terms of the theory of disturbances

$$I_m = \frac{1}{\Phi_0}\int |F|^2 \varkappa^2 \frac{d\Omega_h}{(2\pi)^2}, \quad (9)$$

where

$$F = (\varkappa/2)\int \chi_h(\mathbf{z}) \exp(i\mathbf{g}\mathbf{z})\, d\mathbf{z} \quad (10)$$

$$d\Omega_h = d\Phi_h\, d\theta_h \quad (11)$$

$$\mathbf{q} = \varkappa_2 - \varkappa_1 - \mathbf{K}_2, \quad (12)$$

$\chi_h(\mathbf{z})$ is the Fourier component of the crystal polarizability at point $\mathbf{r}$. In the general case $\chi_h(\mathbf{r})$ varies from point to point owing to bulk and surface defects in

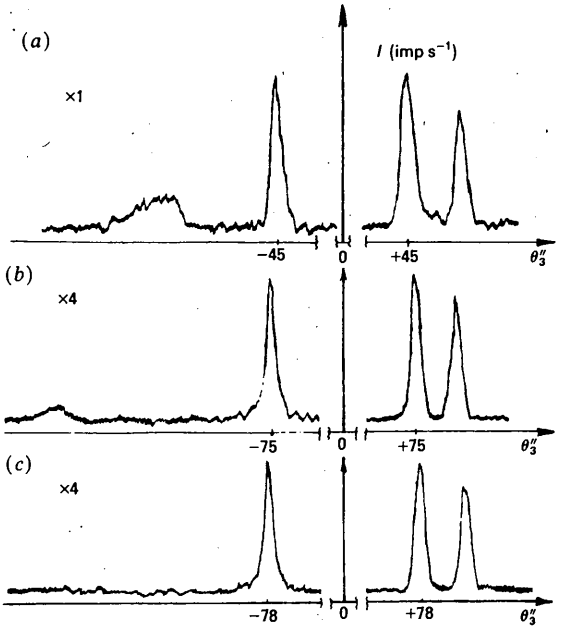

Fig. 2. Experimental TCD spectra at different deviation angles: Si (220), Cu $K\alpha$ radiation, $(+n, -n, +n)$. (*a*) $\theta_2 = \pm 45''$; (*b*) $\theta_2 = \pm 75''$; (*c*) $\theta_2 = \pm 78''$.

the crystal. In the case of an ideal crystal, when $\chi_h(\mathbf{r}) = \chi_h$ and does not depend on $\mathbf{r}$ we can readily find the intensity of the main peak:

$$I_m = \frac{|\chi_h|^2}{4\Phi_0\Phi_h}\frac{1}{\delta^2} \equiv \frac{|\chi_h|^2}{4\Phi_0[(\Phi_h^0)^2-\alpha]^{1/2}}\left[\frac{1}{[(\Phi_h^0)^2-\alpha]^{1/2}-\Phi_h^0}\right]^2. \quad (13)$$

Here

$$P(\alpha) = I_m\delta^2\Phi_h = |\chi_h|^2/4\Phi_0 \quad (14)$$

is constant in an ideal crystal, and it is only due to distortions of the crystal structure that this law might not be observed. Here the characteristic size of the distorted area through depth l_d, which can alter (14), is determined by the value δ (Afanas'ev, Aleksandrov, Imamov, Lomov & Zavyalova, 1983; Yakimov *et al.*, 1984):

$$l_d \simeq 1/\varkappa\delta. \quad (15)$$

At $\Phi_h - \Phi_h^0 \simeq 1°$ we obtain $l_d \simeq 1$ nm. Thus, the present method should be sensitive to the damage in very thin near-surface layers or towards the transition zone boundaries. A similar project was undertaken by Afanas'ev, Aleksandrov, Imamov, Lomov & Zavyalova (1983) and Yakimov *et al.* (1984), in which the dependence of the main peak intensity on the deviation angle of the crystal was studied by the TCD method in the usual Bragg diffraction geometry. A disturbed layer of thickness 1 nm was registered.

The present method, as compared to the conventional one, has distinctive features. First of all, the method is sensitive to the displacements of atoms along the surface, while the conventional scheme is sensitive to displacements perpendicular to the surface. In this aspect the two schemes are complementary to each other. The advantage of the present scheme consists of a much higher intensity of the main peak when the same values of δ are reached. In the standard geometry we have an analogous formula for intensity I_m:

$$I_m = \frac{|\chi_h|^2}{4\sin^2\theta_B}\frac{1}{\delta^2}. \quad (16)$$

Comparing (16) and (13) one can see that in the grazing Bragg–Laue geometry we observe an increase in the intensity by a factor of $\sin^2\theta_B/\Phi_0\Phi_h$, thus the gain in the intensity by a factor of 10^2 is quite feasible.

At small angles $\Phi_0 \sim |\chi_0|^{1/2}$ or $\Phi_h \sim |\chi_h|^{1/2}$ (13) does not hold, because under these conditions the effect of specular reflection should be taken into account. When $|\delta| \gg |\chi_h|^{1/2}$ it is easy to obtain the following expression for I_m:

$$I_m = \frac{|\chi_h|}{4\Phi_0\Phi_h}\frac{1}{\delta^2}\left|\frac{2\Phi_0}{(\Phi_0^2+\chi_0)^{1/2}+\Phi_0}\right|^2 \times \left|\frac{2\Phi_h}{(\Phi_h^2+\chi_0)^{1/2}+\Phi_h}\right|^2, \quad (17)$$

which holds at any angles Φ_0 and Φ_h (χ_0 is the polarizability of the crystal). At $\Phi_0 \gg |\chi_0|^{1/2}$ we have:

$$P(\alpha) = \Phi_h\delta^2 I_m = \frac{|\chi_h|^2}{4\Phi_0}\left|\frac{2\Phi_h}{(\Phi_h^2+\chi_0)^{1/2}+\Phi_n}\right|. \quad (18)$$

As is seen from this formula, $P(\alpha)$ remains a straight line except for a narrow region near $\alpha = \alpha_c$, where a pronounced elevation should appear, which is several times larger than the mean value.

Experimental

The experimental set up is shown in Fig. 1. Unlike the conventional set up for symmetrical Bragg diffraction, the surface of the crystal is placed perpendicular to monochromator and analyzer crystals, although the reflecting planes of all the three crystals, as in the conventional set up, are parallel to each other. To ensure such a position of the studied crystal a special crystal holder, mounted on the goniometer, was prepared. The goniometer rotation ensured the rotation of the studied crystal with an accuracy of up to 0·5″. The crystal holder makes it possible to rotate the crystal in two directions perpendicular to the goniometer with an accuracy of up to 1′. By means of these two rotations the crystal was oriented in such a way that its reflecting planes were parallel to the reflecting planes of the monochromator and analyzer crystals.

The investigation was made on perfect Si single crystals using Cu Kα radiation. For monochromator and analyzer crystals the (110) plane was placed parallel to the surface. The specimen was oriented with the (111) plane parallel to the surface, the reflecting (220) planes making an angle 87·2 (2)° with the surface. The spectra were recorded under the conditions of the Bragg-Laue grazing diffraction at $\Phi_0 < |\Psi|$.

As is seen from Fig. 2, the typical TCD peaks – the main peak and the pseudopeak – are observed on the spectra. However, the positions of these peaks alter with the change in the direction of the deviation angle of the studied crystal. When the crystal deviates to the left by an angle $\alpha = \alpha_c$, the main peak disappears completely, which is in complete agreement with theoretical predictions.

Careful measurements of the position of the main peak were made as a function of θ_2. The results of these measurements are shown in Fig. 3(a). The experimental data confirm theoretical calculations-

the solid curve in Fig. 3 is the calculated position obtained using (6).

The pseudopeak changes its position on the spectrum proportionally to the deviation angle θ_2. That is why at large deviations to the right the pseudopeak can go ahead of the main peak. This case is clearly shown in Fig. 4. As is seen from this figure, at higher θ_2 angles the main peak and the pseudopeak approach each other step by step, and, finally, their angular positions coincide. The further increase of θ_2 changes the sequence of the peaks on the spectrum. The observed curves (Fig. 4) correspond to the angle of incidence $\Phi_0 = 1°$.

At the angle of incidence $\Phi_0 \simeq |\Psi|$ the main peak and the pseudopeaks do not appear at all on the TCD spectra. At positive θ_2, in this case, only the main peak should be evident, whose angular position θ_m is proportional to $\theta_2^{1/2}$. The corresponding spectra are shown in Fig. 5. It is evident from this figure that at $\theta_3 = \pm 15''$ there is a small peak, whose position corresponds to the position of the pseudopeak. This is associated with insufficient collimation of the beam incident on the crystal. The change of the main peak position in the spectrum is shown in Fig. 3(*b*).

The theoretical analysis predicts a dependence of the main-peak intensity on the deviation angle θ_2 [see (14)] for an ideal crystal. This non-trivial and quite unevident dependence was tested experimentally, and the results are presented in Fig. 3(*c*). In accordance with the theory, the observed dependence of the value $P(\alpha)$ on θ_2 formed a straight line within the whole range of angles, with the exception of the region $\alpha = \alpha_c$. A sharp peak on the $P(\alpha)$ curve is observed in the neighborhood of this point, which is evidence of the process of specular reflection of the diffracted wave. This fact is in qualitative agreement with theoretical conclusions.

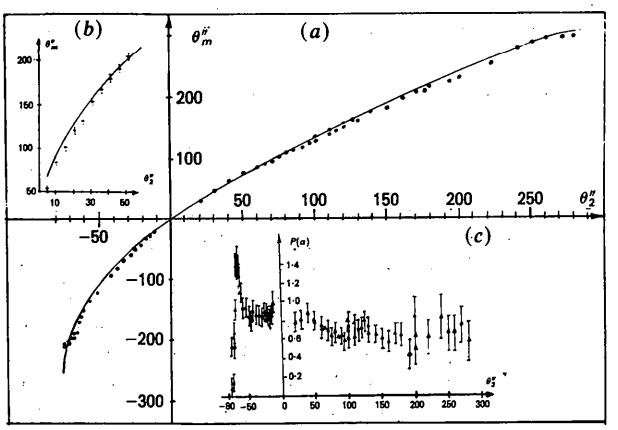

Fig. 3. Position of the main peak in TCD spectra depending on deviation angle θ_2. (*a*) $\Phi_0 \simeq 1°$; (*b*) $\Phi_0 = |\Psi| = 2.2°$. (Solid lines–calculated curves.) (*c*) Experimental dependence of function $P(\alpha)$ on deviation angle θ_2.

Thus, TCD in grazing Bragg–Laue geometry is characterized by a number of peculiarities predicted theoretically and proved experimentally.

1. The main peak vanishes altogether on TCD spectra for negative angles at the deviation angle $\alpha = \alpha_c$.
2. The position of the main peak on TCD spectra corresponds to relation (6).
3. The intensity of the main peak obeys the law (14).
4. Function $P(\alpha)$ has a sharp rise near angle α_c.

Finally, it should be noted that the correspondence of the experimental curve $P(\alpha)$ to (15) testifies to a high perfection of the crystals studied, the thickness of the damaged layer being less than 1 nm.

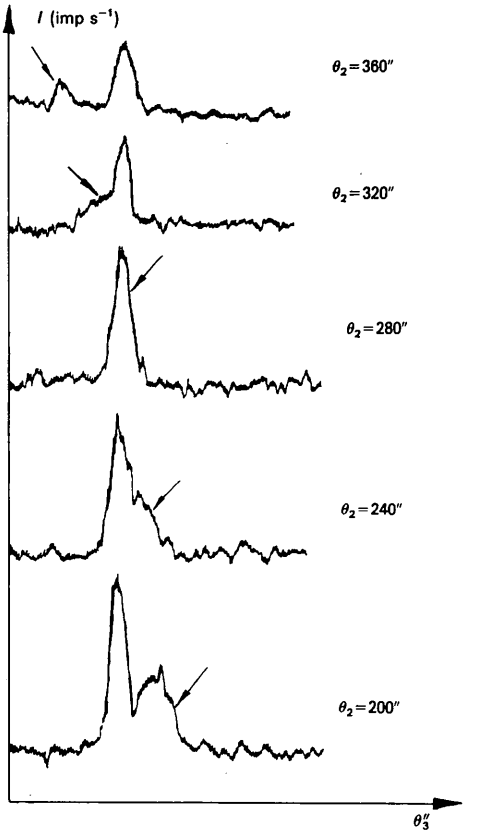

Fig. 4. The pseudopeak outrunning the main peak at higher deviation angle θ_2.

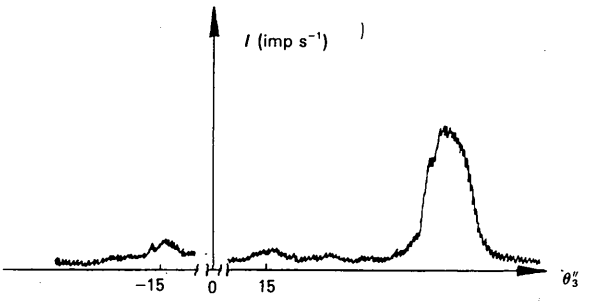

Fig. 5. Experimental TCD spectrum at $\Phi_0 = |\Psi|$; $\theta_2 = 15''$. Si (220), Cu $K\alpha$ radiation, $(+n, -n, +n)$.

References

AFANAS'EV, A. M., ALEKSANDROV, P. A., IMAMOV, R. M., LOMOV, A. A. & ZAVYALOVA, A. A. (1983). Eighth Eur. Crystallogr. Meet., Liège, Belgium, Abstracts, p. 230.

AFANAS'EV, A. M., ALEKSANDROV, P. A., IMAMOV, R. M., LOMOV, A. A. & ZAVYALOVA, A. A. (1984). *Acta Cryst.* A**40**, 352-355.

AFANAS'EV, A. M., ALEKSANDROV, P. A. & MELKONYAN, M. K. (1981). *Kristallografiya*, **26**, 1275-1281.

AFANAS'EV, A. M., IMAMOV, R. M., MASLOV, A. M. & PASHAEV, E. M. (1983). *Dokl. Acad. Nauk SSSR*, **273**, 609-612.

AFANAS'EV, A. M., IMAMOV, R. M., MASLOV, A. M. & PASHAEV, E. M. (1984). *Phys. Status Solidi A*, **84**, 73-78.

AFANAS'EV, A. M., KOVAL'CHUK, M. V., LOBANOVICH, E. F., IMAMOV, R. M., ALEKSANDROV, P. A. & MELKONYAN, M. K. (1981). *Sov. Phys. Crystallogr.* **26**, 13-20.

AFANAS'EV, A. M. & MELKONYAN, M. K. (1983). *Acta Cryst.* A**39**, 207-210.

ALEKSANDROV, P. A., AFANAS'EV, A. M. & STEPANOV, S. A. (1984). *Kristallografiya*, **29**, 197.

BIRGENVAU, R. J., HAMMOUS, E. M., HEINEY, P. & STEPHAUS, R. W. (1980). *Ordering in Two Dimensions*, edited by S. K. SINHA, p. 29. Amsterdam: North-Holland.

EHRHART, P. (1978). *J. Nucl. Mater.* **69&70**, 200.

EISENBERGER, P., ALEXANDROPOULOS, N. G. & PLATZMAN, P. M. (1972). *Phys. Rev. Lett.* **28**, 1519.

EISENBERGER, P. & MARRA, W. C. (1981). *Phys. Rev. Lett.* **46**, 1081.

GOLOVIN, A. L. & IMAMOV, R. M. (1983*a*). *Phys. Status Solidi A*, **77**, K91.

GOLOVIN, A. L. & IMAMOV, R. M. (1983*b*). *Phys. Status Solidi A*, **80**, K63.

HAUBOLD, H. G. & MARTINSEN, D. (1978). *J. Nucl. Mater.* **69&70**, 644.

IIDA, A. (1979). *Phys. Status Solidi A*, **54**, 701-706.

IIDA, A. & KOHRA, K. (1979). *Phys. Status Solidi A*, **51**, 533-542.

LARSON, B. C. & SCHMATZ, W. (1974). *Phys. Rev. B*, **10**, 6, 2307.

LARSON, B. C. & SCHMATZ, W. (1980). *Phys. Status Solidi B*, **99**, 267.

MARRA, W. C., EISENBERGER, P. & CHO, A. Y. (1979). *J. Appl. Phys.* **50**, 6927.

MARRA, W. C., FUOSS, P. H. & EISENBERGER, P. E. (1982). *Phys. Rev. Lett.* **49**, 1169.

NIELSEN, M., ALS-NIELSEN, J., BOHR, J. & MCTAGUE, J. P. (1981). *Phys. Rev. Lett.* **47**, 582.

ROBINSON, I. K. (1983). *Phys. Rev. Lett.* **50**, 1145.

YAKIMOV, S. S., CHAPLANOV, V. A., AFANAS'EV, A. M., ALEKSANDROV, P. A., IMAMOV, R. M. & LOMOV, A. A. (1984). *Pis'ma Zh. Eksp. Teor. Fiz.* **39**, 1, 3-5.

ZAUMSEIL, P. & WINTER, U. (1982). *Phys. Status Solidi A*, **73**, 455.

Acta Cryst. (1985). A**41**, 232-244

On the Maximum-Entropy Estimate of the Electron Density Function

BY JORGE NAVAZA

Laboratoire de Physique, Tour B, Centre Universitaire Pharmaceutique, 92290 Chatenay-Malabry, France

(*Received* 23 *December* 1982; *accepted* 1 *November* 1984)

Abstract

The principle of maximum entropy, considered as a form of statistical inference, is used to obtain an estimate of the electron density function on the basis of partial information. First a maximum-entropy probability distribution of maps, which explicitly takes into account the available information, is obtained, its functional form being a strict consequence of the type of constraint used. Next the electron density function is estimated using this probability distribution. For the particular type of constraint considered here the formulation presented is shown to correspond exactly to a maximum-entropy algorithm using a new form of the configurational entropy of maps.

1. Introduction

Entropy maximization methods have been used in connection with the problem of image reconstruction (Gull & Daniell, 1978). Similar techniques have been used by crystallographers to produce electron density maps (Collins, 1982; Wilkins, Varghese & Lehmann, 1983). The main goal of these methods is to construct maps that use all the available information (*e.g.* diffraction data, positivity of the map) while being maximally noncommital to any other information. Different expressions for the entropy have been used (see *e.g.* Frieden, 1972; Abels, 1974), which were associated, sometimes in a non-explicit way, with different assumptions.

In this paper we use a statistical approach and information theory to produce a maximum-entropy estimate of the electron density function. A maximum-entropy probability distribution of maps that explicitly takes into account the available information will be obtained starting from first principles. The statistical entropy of this probability distribution will then be calculated, its functional form being a strict consequence of the constraint imposed on the sought map. In particular, if the constraints are functionals of the estimated map, the statistical entropy is itself a functional of it and is called the configurational entropy of the map. For certain types of constraints we find the forms used by other authors

0108-7673/85/030232-13$01.50